Journal of Power Sources 263 (2014) 52–58

Contents lists available at ScienceDirect

Journal of Power Sources

journal homepage: www.elsevier.com/locate/jpowsour

New battery strategies with a polymer/Al_2O_3 separator

Kyusung Park [a], Joon Hee Cho [b], Kadhiravan Shanmuganathan [b], Jie Song [a], Jing Peng [c], Mallory Gobet [c], Steven Greenbaum [c], Christopher J. Ellison [a,b], John B. Goodenough [a,*]

[a] Texas Materials Institute, The University of Texas at Austin, Austin, TX 78712, United States
[b] McKetta Department of Chemical Engineering, The University of Texas at Austin, Austin, TX 78712, United States
[c] Department of Physics & Astronomy, Hunter College of The City University of New York, New York, NY 10065, United States

HIGHLIGHTS

- Al_2O_3/PEO composite film was fabricated as a battery electrolyte membrane.
- The membrane is thin, flexible, and mechanically robust.
- The membrane can block Li/Na dendrites and enable assembly of charged-state batteries.
- A hybrid redox-flow battery could be achieved by using the membrane together with a PEDOT:PSS-coated polypropylene separator.
- Osmosis issues could be minimized by balancing the solute concentrations of catholyte and anolyte.

GRAPHICAL ABSTRACT

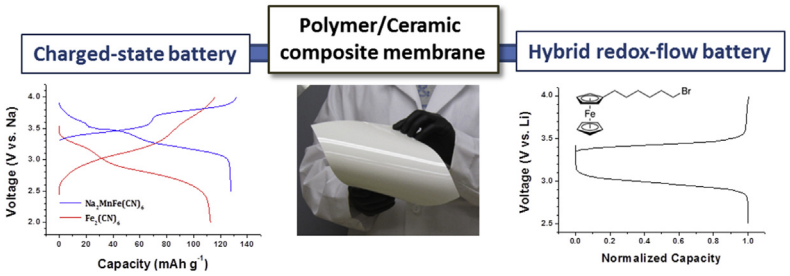

ARTICLE INFO

Article history:
Received 10 February 2014
Received in revised form
3 April 2014
Accepted 4 April 2014
Available online 14 April 2014

Keywords:
Ceramic–polymer composite membrane
Charged battery
Hybrid redox flow battery
Osmosis

ABSTRACT

A low-cost, thin, flexible, and mechanically robust alkali-ion electrolyte separator is shown to allow fabrication of a safe rechargeable alkali-ion battery with alternative cathode strategies. A Na-ion battery with an insertion host as cathode and a Li-ion battery with a redox flow-through cathode are demonstrated to cycle without significant fade. The separator membrane is a composite of Al_2O_3 particles and cross-linked ethylene-oxide chains; it can be fabricated at low cost into a large-area thin membrane that blocks dendrites from an alkali-metal anode. To block a soluble ferrocene redox molecule from crossing from the cathode side to the anode in a Li-ion battery with a redox-flow cathode, a thin mixed Li^+/electronic-conducting film has been added to the cathode side of the composite separator. An osmosis issue was minimized by balancing concentrations of solutes on the two sides of the separator where the cathode side contains a soluble redox molecule.

1. Introduction

A sustainable modern society will require massive use of variable renewable energy sources; wind and solar energy. A corollary is that electrical energy generated by wind and solar farms must be stored for at least 24 h, and the most versatile energy storage mode is chemical energy. Rechargeable batteries store chemical energy in their electrodes. Electric cars powered by batteries offer distributed energy storage and removal of a distributed source of air pollution. Stationary batteries can complement the grid for storage of electrical energy generated by wind and/or solar farms. However, the energy stored in a typical

* Corresponding author.
E-mail address: jgoodenough@mail.utexas.edu (J.B. Goodenough).

http://dx.doi.org/10.1016/j.jpowsour.2014.04.017
0378-7753/

rechargeable battery cell is relatively small, which is why today's batteries do not compete with the energy stored in a fossil fuel. But the societal cost to the environment of our extensive use of fossil fuels can no longer be hidden from the individual consumer. Therefore, it has become an imperative that a way be found to increase the energy density of a rechargeable battery cell at lower cost. Increasing the energy density of a rechargeable cell requires development of a cell design that goes beyond the limitations of present-day Li-ion batteries. In this paper we demonstrate the feasibility of such a cell design.

The key component of the alternative cell design presented in this paper is a solid separator membrane that blocks dendrites from an alkali-ion anode and soluble redox species in the cathode side from crossing over to the anode. The separator membrane must be capable of low-cost fabrication into large-area sheets that are thin, mechanically robust, and preferably flexible. Such a membrane would allow assembly of a charged cell, which eliminates capacity loss from the cathode on the initial charge of a cell assembled in a discharged state; it would also increase the voltage for a given cathode and allows alternative cathode strategies. We demonstrate the feasibility of this design with a composite membrane composed of Al_2O_3 and a polyethylene oxide (PEO)-based polymer on which a thin conductive film may be added to the cathode side of the membrane: a Na-ion cell with an insertion cathode and a Li-ion cell with a liquid redox-flow cathode illustrate the feasibility of the design.

2. Experimental

2.1. Membrane fabrication

2.1.1. Materials

Azobisisobutyronitrile (AIBN, thermal initiator), Pentaerythritol tetrakis (3-mercaptopropionate) (PETT, M_n = 489 g mol^{-1}), and Poly(3,4-ethylenedioxythiophene):poly(styrenesulfonate) (3.0–4.0 wt.% in H_2O) were purchased from Sigma Aldrich and used as received. Di(ethylene glycol) divinyl ether (DEGDVE, molecular weight = 158 g mol^{-1}) was provided by BASF, Germany and used as received. Aluminum oxide (Al_2O_3) (particle size: 300–400 nm, Alfa Aesar) was used after drying at 400 °C for 1 day in an oven.

2.1.2. Preparation of the ceramic/polymer composite membrane

PETT and DEGDVE were mixed at an equimolar ratio of functional groups and AIBN was dissolved in DEGDVE at 1 wt.% (based on total weight of PETT and DEGDVE) prior to the mixing to avoid premature cure. A low molecular weight telechelic precursor such as a DEGDVE was chosen to ensure dimensional stability after swelling in a battery electrolyte. Al_2O_3 nanoparticles were finally added in the designed weight ratio (PETT and DEGDVE:Al_2O_3 = 2:1) after grinding to remove macroscopic aggregation. The solution was shaken by a vortex mixer (Thermolyne 37600) for 5 min and then vigorously stirred for 5 min to uniformly disperse Al_2O_3 nanoparticles in the mixture of PETT and DEGDVE. All these mixing procedures were carried out in a UV-light-free environment to minimize reaction of the thiol-ene system. The solution was quickly transferred to a mold and then baked in an oven. The composite film with thickness of 0.75 mm was cured at 80 °C for 4 h and postcured at 100 °C for 2 h. The postcuring was carried out to ensure the complete depletion of initiator; it was performed under vacuum to suppress oxidation of the film at high temperature. The cross-linked composite film was removed from the mold and used after drying in vacuum at room temperature overnight. In addition, the PETT–DEGDVE neat film was synthesized with a similar procedure without Al_2O_3 nanoparticles.

2.1.3. Differential scanning calorimetry (DSC)

Samples were scanned from −100 °C to 200 °C at a heating rate of 5 °C min^{-1} under a nitrogen purge (50 mL min^{-1}) using a Mettler Toledo DSC 1. The glass transition temperature (T_g) was taken as the midpoint of the specific heat increment from the second heating cycle and the melting temperature (T_m) was taken from the endothermic peak during the second heating run. The percent crystallinity of the samples was estimated based on the heat of fusion of 100% crystalline PEO (51 cal g^{-1}) [1].

2.1.4. Mechanical property evaluation

Stress–strain behavior of the polymer electrolytes was analyzed with a tensile tester (Micro Tensile Tester 5848, Instron). Dogbone-shaped specimens were prepared with a mold with dimensions of 38.0 mm in length, 5.0 mm in width, and 1.0 mm in thickness. A 1 kN load cell was used and samples were extended at a strain rate of 1.0 mm min^{-1}.

2.1.5. Poly(3,4-ethylenedioxythiophene):poly(styrenesulfonate) (PEDOT:PSS) thin films on polypropylene (PP) separator

The PP separator (Celgard 2500) was treated with oxygen plasma to increase its surface energy so that an aqueous solution of PEDOT:PSS may spread well on the surface. PEDOT:PSS thin films (thickness: 153 nm) were spin-coated (4500 rpm, 30 s) on the PP separator from an aqueous solution (3.0–4.0 wt.%) and then dried at 75 °C for 5 h under vacuum. PEDOT:PSS thin films were prepared on glass slides under the same condition and used for the measurement of film thickness. The thickness of the films was measured at multiple locations on each sample with a profilometer (Dektak 6M Stylus Profiler, Veeco Instruments Inc.).

2.2. NMR test

2.2.1. Sample preparation

Four membrane samples were soaked in 1 M LiTFSI in EC/DEC (1/1 in volume). The Al_2O_3/PEO membrane was soaked for 24 h, and the other three samples were soaked for 1 min each. Because of solvent loss upon transfer to the NMR tube, another strategy was adopted: the Al_2O_3/PEO membrane was placed inside the NMR tube and a preweighed amount of electrolyte was injected into the tube immediately prior to sealing and equilibrated for 24 h. All procedures were performed in an Ar glove box. The NMR spectra and diffusion profiles indicated a homogeneous distribution of electrolyte within the membrane.

2.2.2. Diffusion coefficient measurement

300 MHz spectrometer with a DOTY Z-gradient diffusion probe was used. All experiments were performed at room temperature (23 °C). The stimulated echo pulse sequence was used [2]. We used the following formula to calculate the diffusion coefficient D.

$$I = I_0 \exp\left[D\gamma^2\delta^2 g^2\left(\Delta - \frac{\delta}{3}\right)\right]$$

Where γ is gyromagnetic ratio of the studied nucleus, g is the gradient strength (ranging from 2 to 1150 G cm^{-1}), δ the gradient pulse duration (1.5–2 ms) and Δ the diffusion delay (70–200 ms).

2.3. Powder synthesis

2.3.1. Na-ion battery cathode materials

$Fe_2(CN)_6$ and $Na_2MnFe(CN)_6$ were prepared by a precipitation method. For $Fe_2(CN)_6$, a $K_3Fe(CN)_6$ aqueous solution was slowly added to a $FeCl_3$ aqueous solution under continuous stirring; the molar ratio of $K_3Fe(CN)_6$: $FeCl_3$ was controlled to 1:2. The resulting

solution was maintained at 60 °C for 6 h, and the as-obtained dark green precipitate was filtered, rinsed twice with deionized water and once with acetone, and finally dried in air at 60 °C overnight.

For $Na_2MnFe(CN)_6$, 2.30 g $Mn(NO_3)_2$ solution (50 wt.%) was dissolved into 50 mL deionized water, and 1.42 g $Na_4Fe(CN)_6$ was dissolved into 100 mL water. 14 g NaCl was added into the $Na_4Fe(CN)_6$ solution. $Mn(NO_3)_2$ solution was added dropwise into the NaCl/$Na_4Fe(CN)_6$ solution under magnetic stirring. The suspension was aged for 2 h before being filtered. The white precipitate was washed with deionized water several times and then dried at 120 °C for 8 h.

2.4. Electrochemical tests

2.4.1. Na-ion battery cell test

The electrodes were prepared by rolling a mixture of 60% active material, 30% carbon black and 10% polytetrafluoroethylene (PTFE) into a thin film. The electrolyte is 1 M $NaClO_4$ in ethylene carbonate/diethyl carbonate (EC/DEC, 1/1 in volume) solution. $Na_2MnFe(CN)_6$ was charge/discharged at 0.1 C and then 1 C current for 200 cycles in the voltage range of 2.5–4.0 V (1 C = 120 mA g^{-1}). $Fe_2(CN)_6$ was charged/discharged at 0.1 C and then 2 C current for 400 cycles in the voltage range of 2.0–4.0 V. For the cycle tests, two different types of separators were adopted. As a standard reference, a glass fiber paper (Whatman) was used as a separator. In the case of the Al_2O_3/PEO membrane, it was soaked in 1 M $NaClO_4$ in EC/DEC (1/1) for 1 day prior to the tests. The Al_2O_3/PEO membrane had a thickness of 0.75 mm and it was not optimized for a Na-ion cell test.

2.4.2. Symmetric cell test

A symmetric cell with Li metal on both sides of an electrolyte membrane was assembled to check the chemical and electrochemical stability of the interface of a Li/electrolyte membrane. The Al_2O_3/PEO membrane was presoaked in 1 M lithium bis(trifluoromethane)sulfonamide (LiTFSI) in EC/DEC (1/1 in volume) for the cell operation. A Li|Al_2O_3/PEO|Li symmetric cell was cycled at a current of 0.02 mA for 5 h in each charge and discharge. The cell was fully charged up to 4 V vs. Li after 11 cycles of the charge/discharge to check whether the Al_2O_3/PEO membrane can block lithium dendrites. The surface of the membrane was inspected with an optical microscope after disassembling the charged test cell.

2.4.3. Dual electrolyte cell test

A Swagelok-type test cell is used for the electrochemical tests of the dual electrolyte cell system, which is a redox flow battery cell in a static mode. The base electrolyte for catholyte and anolyte is 1 M LiTFSI in EC/DEC (1/1 in volume). 6-Bromohexyl ferrocene was adopted as a redox molecule for the catholyte, and 0.1 M of the molecule was dissolved in the base electrolyte. In the case of balancing the solute concentrations between catholyte and anolyte, some spectator molecules with the same concentrations as the cathode redox molecule were added to the anolyte such as 1-butyl-1-methylpyrrolidinium bis(trifluoromethylsulfonyl)imide and poly(ethylene glycol) dimethyl ether (PEGDME, average molecular weight ~500 g mol^{-1}).

The counter electrode was a lithium-metal foil that is mounted on a stainless-steel rod, and the Al_2O_3/PEO membrane was placed on top of the lithium anode. The Al_2O_3/PEO membrane was soaked with liquid anolyte for 1 day before cell assembly. A poly(vinylidene fluoride-*co*-hexafluoropropylene) (PVDF-HFP; Aldrich, average M_w ~ 400,000) gel polymer electrolyte was placed in between the Li and the Al_2O_3/PEO membrane to keep the anolyte during cycling and to reduce interfacial resistance. The PEDOT:PSS-coated PP separator was be placed on the catholyte side of the Al_2O_3/PEO membrane to block the crossover of the catholyte redox molecules. For the cathode current collector, carbon felt filled the catholyte chamber, which was further connected to an external load via a stainless-steel rod. The cell was galvanostatically charged/discharged in the voltage range of 2.7–3.7 V vs. Li at a current density of 0.1 mA cm^{-2}.

3. Results and discussion

3.1. The membrane

A thin, mechanically robust membrane that blocks dendrites from an alkali-ion anode can be fabricated at low cost as an oxide/polymer composite. Our initial attempts to fabricate such a composite with a solid Li^+ electrolyte $Li_{7-x}La_3Zr_{2-x}Ta_xO_{12}$ showed that the garnet had a large impedance for Li^+ transfer across the garnet/liquid–electrolyte interface; the garnet surface is readily attacked by Na and by moisture and CO_2 on exposure to air. Therefore, we chose to use Al_2O_3 as the oxide and a PEO-based polymer that is porous to the liquid electrolyte. Loading of the membrane with sufficient Al_2O_3 to block dendrites from the anode still allowed fabrication of a thin, flexible, mechanically robust membrane once thiol-ene chemistry was introduced to make a uniform PEO-based polymer structure with a thiol crosslinker. Thiol-ene chemistry provides a highly efficient and simple method of preparing crosslinked films with superior mechanical properties [3]. It has received great attention from industry because of its rapid polymerization rates in air to form homogeneously crosslinked networks with only a small concentration of relatively benign initiators [4,5]. The thiol-ene chemistry gives high conversion of virtually any -ene precursor with low shrinkage and stress [6]. Vinyl ether is especially preferable among various -enes because thiol-vinylether polymerization involves, ideally, a pure step-growth thiol-ene reaction without homopolymerization and produces exceptionally uniform crosslink density with few dangling chain ends [6].

In order to prevent redox-molecule crossover from the cathode side to the anode, it is important to restrict homopolymerization and the polymer network molecular weight between crosslinks (M_c). Di(ethylene glycol) divinyl ether (DEGDVE) with ethylene-oxide (EO) units and penterythritol tetrakis (3-mercaptopropionate) (PETT) as a crosslinker were used in the polymer membrane fabrication. An Al_2O_3/PETT–DEGDVE (denoted as Al_2O_3/PEO hereafter) composite membrane was prepared by thermally initiated thiol-ene polymerization [5,7], which follows a step-growth mechanism (Fig. 1a) [6]. The polymer electrolytes were rapidly fabricated with inexpensive chemicals in quantitative yield under mild conditions without the use of a solvent, thus requiring essentially no clean up. The low-cost, environmentally friendly, and facile preparation of the membrane should allow

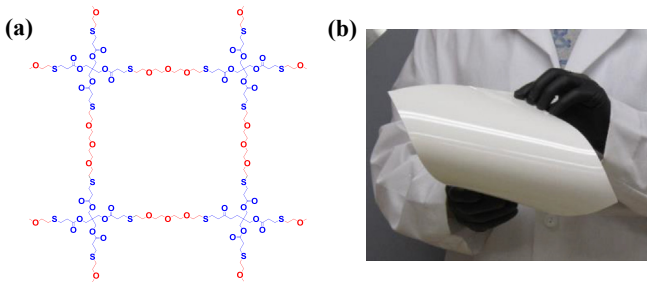

Fig. 1. (a) Crosslinked PETT–DEGDVE polymer chain structure in the Al_2O_3/PEO membrane and (b) a photograph of the membrane (25 × 20 cm^2).

large-scale industrial use. Large-area, uniform and flexible membranes were easily obtained (Fig. 1b).

The glass transition temperature (T_g) of the Al_2O_3/PEO composite was −30 °C, and a very small endothermic peak consistent with a melt transition temperature (T_m) was observed at 63 °C. The associated crystallization peak was not observed on cooling below T_m. The fractional crystallinity of the Al_2O_3/PEO composite was 0.2%, which indicates the polymer networks consist predominantly of an amorphous phase. The homogeneous and high-density crosslinking between the small molecular weight PEO-based monomer units effectively inhibits the crystallization of the polymer membrane. Along with the amorphous polymer structure, the T_g well-below room temperature facilitates the incorporation of liquid electrolyte in the polymer network. It is worth noting that the dimensional stability of this membrane will be defined by the thermal stability of the covalent molecular network (*i.e.* >250 °C). This stability is unlike traditional porous battery separators (*e.g.* polyethylene and polypropylene) whose upper use temperatures are fixed by T_m (*e.g.* ~120 °C) [8].

The Al_2O_3/PEO membrane is permeable to Li^+ after it is soaked with battery liquid electrolyte prior to electrochemical tests (Table 1). Since the membrane is not a dry solid state electrolyte, it is not necessary to activate thermally the Li^+ mobility. Previous researchers have made a Li salt-loaded dry polymer electrolyte without Al_2O_3 loading with thiol-ene chemistry, but it requires thermal activation to achieve a high Li^+ conductivity [9]. After soaking in the electrolyte, the membrane remains flexible and smooth without any Al_2O_3 loss (Fig. 2). The compact polymer mesh binds the Al_2O_3 powder strongly, which is beneficial to the mechanical integrity of the composite membrane.

Solvent and ionic mobilities in the Al_2O_3/PEO membrane containing ~42 wt.% 1 M lithium bis(trifluoromethylsulfonyl)imide (LiTFSI) in ethylene carbonate/diethyl carbonate (EC/DEC, 1/1 in volume) electrolyte were assessed by NMR pulsed gradient stimulated echo measurements [10]; ^1H for the carbonate solvents, ^7Li and ^{19}F for the cations and anions, respectively (Table 2). All measurements were performed at ambient temperature (23 °C). As with most electrolytes, whether liquid carbonate, gel, or polymer, the anions are characterized by significantly higher diffusivity than the cations. In the present case, the lithium and TFSI diffusion coefficients are 5.5×10^{-13} and 2.4×10^{-12} m^2 s^{-1}, respectively. The anion diffusivity is comparable to the average (for EC and DEC) molecular solvent diffusivity of 3×10^{-12} m^2 s^{-1}. Despite the relatively low Li (and TFSI) diffusivity, as compared with values for conventional polypropylene (PP) separator (Celgard 2500) or gel-polymer (poly(vinylidene fluoride-*co*-hexafluoropropylene), PVDF-HFP copolymer) soaked with electrolyte, which are two orders of magnitude higher, the Al_2O_3/PEO membrane can be made sufficiently thin to have adequate conductance and still maintain its mechanical integrity. In the case of the other polymers, however, it must be mentioned that their electrolyte uptake can be more than an order of magnitude greater than in the Al_2O_3/PEO membrane, which also compromises their mechanical properties.

Table 1
Electrolyte uptake of different membranes.

Sample	Before soaking, g	After soaking, g	Weight, g (absorbed electrolyte)	$(W_{wet} - W_{dry})/W_{dry}$, %
Al_2O_3/PEO	0.236	0.338	0.102	43.4%
Celgard 2500	0.044	0.154	0.111	253%
PEDOT:PSS-coated Celgard	0.049	0.160	0.112	230%
PVDF-HPF	0.050	0.625	0.575	1160%

Table 2
NMR data analysis and measured diffusion coefficients.

Sample	Nucleus	D (m^2 s^{-1}) (component 1)	(Comp 1 weighting)	D (m^2 s^{-1}) (component 2)	(Comp 2 weighting)
PEO/Al_2O_3 membrane	^1H	1.85E-11	0.630	2.90E-12	0.370
	^{19}F	2.40E-12			
	^7Li	5.49E-13			
Celgard 2500 separator	^1H	1.35E-10	0.722	1.69E-11	0.278
	^{19}F	1.29E-10			
	^7Li	4.66E-11			
PEDOT:PSS-coated Celgard	^1H	7.11E-10	0.832	1.29E-10	0.168
	^{19}F	1.43E-10			
	^7Li	1.06E-10			
PVDF-HFP membrane	^1H	2.33E-10	0.647	4.63E-11	0.353
	^{19}F	8.87E-11			
	^7Li	6.25E-11			

The Li^+-permeable Al_2O_3/PEO membrane was subjected to a mechanical stability test (Fig. 3); tensile strength and elongation at break were assessed. The PEO-based polymer (PETT–DEGDVE) membrane without Al_2O_3 shows a 5.5% elongation under a 0.76 MPa tensile load without plastic deformation before fracture. The Al_2O_3/PEO membrane fractured at 2.7 MPa after a 5.5% elongation, which is a reasonable value as a membrane. We wish to note here that the membrane is very flexible and robust. These two key properties for this application may not be reflected directly from

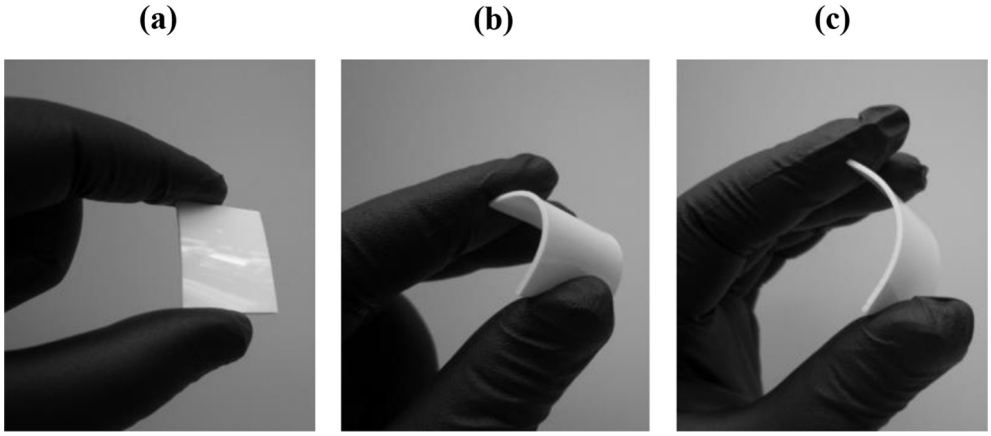

Fig. 2. Photographs of the Al_2O_3/PEO composite membrane (30 × 20 × 1 mm^3) (a) before and (b) after bending in a dry state, and (c) after soaking in dimethyl carbonate (DMC) solution for 1 day.

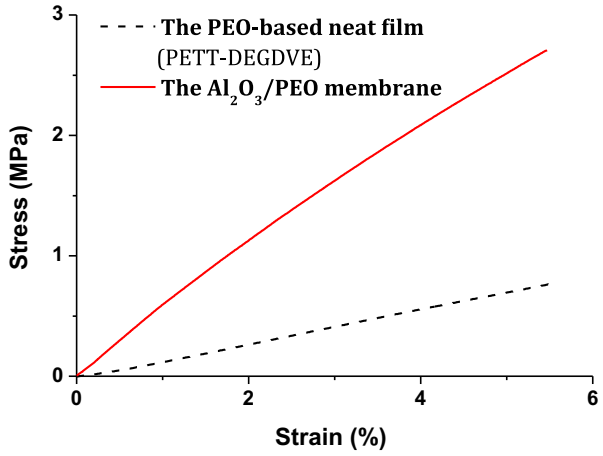

Fig. 3. Stress-strain behaviors of the neat PEO-based network (PETT–DEGDVE; black dotted line) and the Al_2O_3/PEO membrane (red solid line) in a tensile mode.

the values mentioned above, but they are very evident from the pictures and data contained herein.

A critical safety issue is whether the membrane can block dendrite penetration from an alkali anode during cycling. A symmetric Li|Al_2O_3/PEO|Li cell was galvanostatically charged/discharged at 0.02 mA (Fig. 4) for 5 h with no overvoltage increase, showing reversible Li^+ transport and a stable membrane/Li interface. The cell was then fully charged to generate extensive Li dendrites on one side of the membrane. The dendrites dented the membrane surface, but did not penetrate the membrane. This impressive result was further confirmed by an electrochemical-cell test in a Na cell, which provided a severe dendrite condition.

4. Battery demonstration

4.1. A Na-ion battery

Since the membrane also transports Na^+, we prepared a charged half cell with a Na anode and, as cathode, a transition-metal cyanide with a Prussian-blue cyano perovskite structure that allows a Na insertion/extraction reaction [11,12]. In a conventional half-cell with a porous glass-fiber separator, dendrites from the sodium anode penetrate the separator to short-circuit the cell after a relatively few cycles. Therefore, as a model test that Na dendrites are blocked by the Al_2O_3/PEO membrane, half-cell tests with this membrane were compared with those with a conventional separator. No attempt was made to optimize the Al_2O_3/PEO membrane for a Na-ion battery; it was simply soaked with the liquid Na^+ electrolyte 1 M $NaClO_4$ in EC/DEC (1:1). Fig. 5 compares the charge/discharge performance of half-cells with $Na_2MnFe(CN)_6$ and $Fe_2(CN)_6$ with the Al_2O_3/PEO and a conventional glass-fiber separator. For the $Fe_2(CN)_6$ cathode, the redox voltages at 3.74 and 3.47 V vs. Na on charge and 3.10 and 2.78 V on discharge correspond to the oxidation/reduction of the low-spin and high-spin Fe^{3+}/Fe^{2+} redox couples, respectively. For the $Na_2MnFe(CN)_6$ cathode, the 3.52/3.85 V and 3.27/3.57 V plateaus in the first cycle can be assigned to the low-spin Fe^{3+}/Fe^{2+} and high-spin Mn^{3+}/Mn^{2+} couples, respectively. The Al_2O_3/PEO membrane is seen to improve the cycle performance significantly. Even after 400 cycles, there was no capacity fade with $Fe_2(CN)_6$ as cathode. The initial capacity at 2 C is 75.3 mAh g^{-1} and the 400th capacity is 75.6 mAh g^{-1} with the Al_2O_3/PEO membrane whereas with the glass-fiber separator it drops from 71.3 to 21.8 mAh g^{-1}. The high-rate capacity values also suggest that the Al_2O_3/PEO membrane doesn't impede Na^+ transport compared to the glass-fiber separator with highly open microstructure.

4.2. Redox-flow Li-ion battery

A redox-flow battery (RFB) has a soluble molecule in a liquid cathode; the redox molecules flow past a porous electronic conductor to make electronic contact with the cathode current collector [13]. In this high-capacity battery, the separator membrane must also block the soluble redox molecules from crossing over to the anode. For an initial test of an RFB, we used the bare Al_2O_3/PEO membrane and chose 6-bromohexyl ferrocene as the redox molecule with the expectation that this molecule would be large enough to be blocked from passing through the pores of the membrane. The 6-bromohexyl ferrocene was chosen as the redox molecule because (1) it is liquid, (2) ferrocene is an electrochemically stable redox molecule at an attractive energy, and (3) the hydrophobic alkyl chain was attached to increase the size of the molecule. The Al_2O_3/PEO membrane was soaked with 1 M LiTFSI in EC/DEC for 1 day prior to cell assembly. Fig. 6a shows the charge/discharge curves of this cell; they show a single voltage plateau at about 3.1 V vs. Li during discharge. However, the capacity fades rapidly and the overvoltage increases significantly with cycling. A postmortem analysis showed that the anolyte had moved to the catholyte side to dry up the anolyte side and the redox molecule had moved to the anode to cover the lithium with decomposition products (Fig. 6b).

This test revealed two problems: the membrane pores are too large to block crossover by the redox molecule and osmosis occurs across the membrane. A mathematical estimation of the size of the stretched polymer mesh between two neighboring crosslinks is about 30.14 Å [14,15], which is not small enough to block the catholyte redox molecule (Fig. 1a). The high concentration of the large redox molecule in the catholyte with no additives in the anolyte was responsible for the osmosis.

We adopted two strategies to address these problems: (1) large spectator molecules, *e.g.* ionic liquids and soluble polymers, were

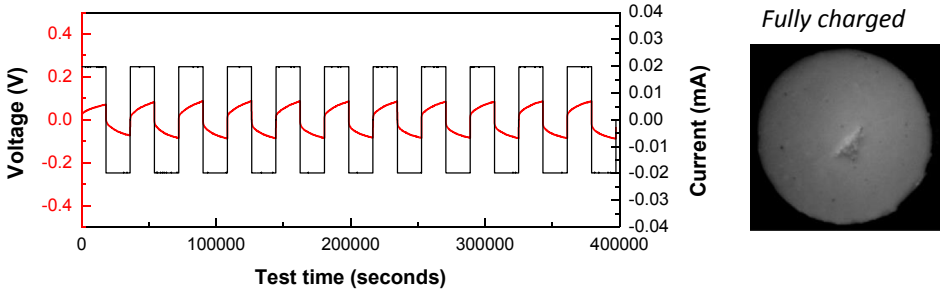

Fig. 4. Galvanostatic charge/discharge voltage curves of a Li|Al_2O_3/PEO|Li symmetric cell at the current of 0.02 mA at room temperature. The Al_2O_3/PEO membrane was soaked with 1 M LiTFSI in EC/DEC (1/1 in volume) for 1 day. A photograph shows surface morphology of the Al_2O_3/PEO membrane after contact with electrochemically grown Li dendrites.

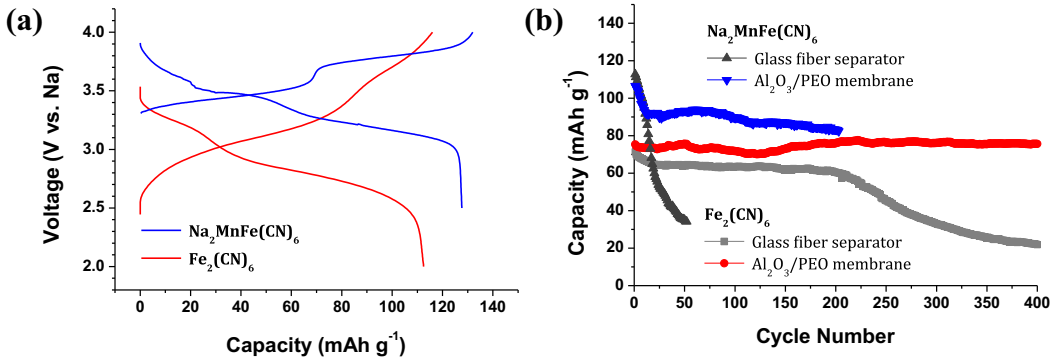

Fig. 5. (a) Charge/discharge voltage curves of $Na_2MnFe(CN)_6$ and $Fe_2(CN)_6$ and (b) their cycle performances with a glass fiber separator and the Al_2O_3/PEO membrane soaked with 1 M $NaClO_4$ in EC/DEC (1/1) liquid electrolyte.

introduced into the anolyte to balance the concentrations of the solutes in the anolyte and catholyte; (2) a thin film of a mixed electronic/Li^+ conductor was added to the cathode side of the Al_2O_3/PEO membrane to block the flow-through catholyte molecule from crossing the membrane. For example, the ionic liquid l-butyl-1-methypyrrolidinium bis(trifluoromethylsulfonyl)imide in the anolyte at a balanced concentration stabilizes the capacity fade after 25 cycles (not shown here). Different diffusion kinetics of the ionic liquid and the catholyte redox molecule in the membrane may have been responsible for not totally eliminating the osmosis issue; but after kinetic equilibrium was reached, the cell showed an acceptable cycle life. The thin film added to the cathode side of the membrane must leave the membrane flexible and be uniform with no defects. We reported several $LiFePO_4$ composite electrodes with polypyrrole or amorphous VO_x [16,17]; these mixed electronic/Li^+ conductors improved the electrode kinetics. These previous tests inspired us to test also these films deposited on PP-based porous battery separators. First, VO_x was coated homogeneously on a PP separator after forming an adhesive layer of polydopamine on the PP membrane. However, different wetting behaviors between VO_x and the polymer in the presence of the liquid electrolyte prevented good adhesion of the thin film. Therefore, a conducting polymer, poly(3,4-ethylene dioxythiophene):poly(styrene sulfonate) (PEDOT:PSS), was coated on the PP separator by spin coating. The hydrophobic nature of the PP separator requires a pretreatment with oxygen plasma to make its surface hydrophilic. The concentration of the polymer solution and the spinning speed were controlled to form a thin and uniform film without any macro/micro holes as shown in Fig. 6c. The thickness of

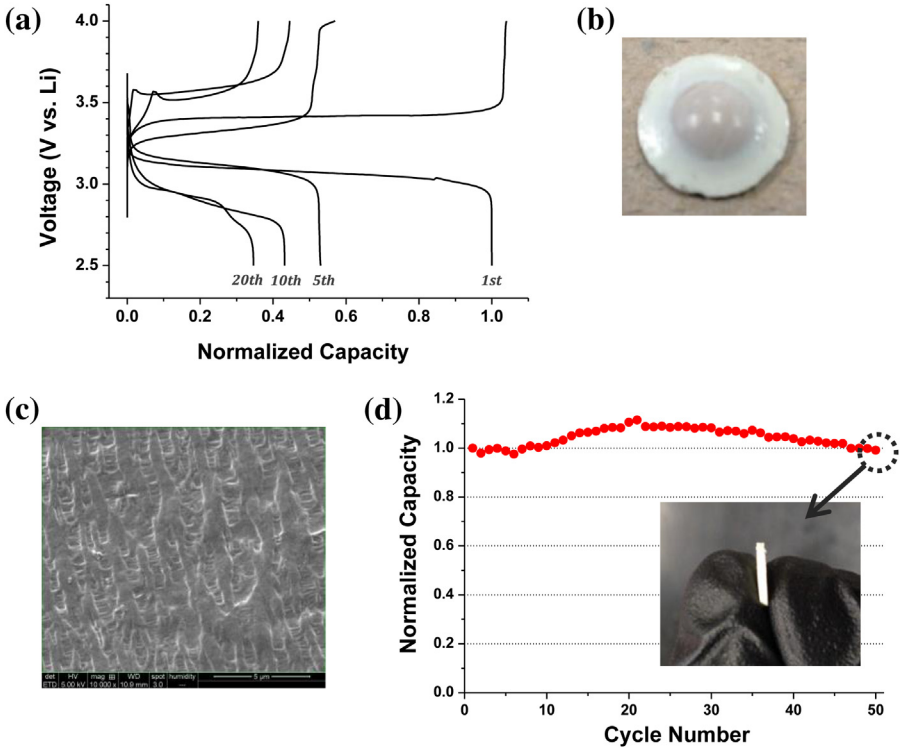

Fig. 6. (a) Charge/discharge voltage curves of a 6-bromohexyl ferrocene catholyte/Li cell separated by the Al_2O_3/PEO membrane soaked with electrolyte. The base electrolyte is 1 M LiTFSI in EC/DEC (1/1), and the anode is lithium metal. (b) Anode side photograph of the Al_2O_3/PEO membrane after cycling. (c) Surface morphology of the PEDOT:PSS-coated polypropylene separator (PP; Celgard 2500). (d) Charge/discharge cycle performance of the 6-bromohexyl ferrocene catholyte with the Al_2O_3/PEO membrane and the PEDOT:PSS-coated PP separator. Anolyte concentration was balanced with PEGDME (molecular weight ~500 g mol^{-1}).

the PEDOT:PSS film was ~150 nm. The PP separator kept its microporous structure through the process of coating the thin PEDOT:PSS film. A defect-free PEDOT:PSS film was then introduced on the cathode side of the Al_2O_3/PEO membrane, and the cell was discharged/charged galvanostatically. Fig. 6d shows the cycle life of the cell with the double-membrane configuration. Poly(ethylene glycol) dimethyl ether (PEGDME, average molecular weight $\simeq$500 g mol^{-1}) was added to the anode electrolyte to balance the solute concentrations between catholyte and anolyte. The conducting polymer thin film is seen to block crossover of the 6-bromohexyl ferrocene molecule from the catholyte to provide a stable cycle life without capacity fade for 50 charge/discharge cycles. After cycling, the cell was disassembled and the Al_2O_3/PEO membrane was cut to check its cross section to see whether there was any color change owing to crossover of the redox molecule. As shown in Fig. 6d, the membrane cross section remained white, which confirms no crossover of the ferrocene molecule. These results show that a combination of the Al_2O_3/PEO membrane and a PEDOT:PSS thin film can provide a thin, flexible, scalable, mechanically robust, and low-cost membrane for assembling a redox-flow battery with a lithium or a sodium anode.

5. Conclusion

The development of a low-cost separator membrane that blocks dendrites from an alkali-metal anode from reaching the cathode and a soluble redox molecule on the cathode side from reaching the anode opens up the possibility of achieving rechargeable batteries of higher power density for portable power in an electric vehicle and large-capacity storage of electricity from renewable, but variable energy sources. Development of a Li–S or a Na–S battery also shows promise, but it requires a thin film that can block completely the smaller Li_2S_x ($2 < x \leq 8$) soluble redox molecules. Development of a Li-air cell may require a hydrophobic all-oxide film on the cathode side.

Acknowledgments

JBG acknowledges support from the Welch Foundation (Grant F-1066) and the Lawrence Berkeley National Laboratory BATT Program (project number 6998655). CJE acknowledges partial support from the Welch Foundation (Grant F-1709), 3M Nontenured Faculty Grant and DuPont Young Professor Award. JHC acknowledges partial financial support from LG Chem. Graduate Research Fellowship. NMR measurements at Hunter College were supported by Grant # DE-SC0005029 from the Basic Energy Sciences Division of the U.S. Department of Energy.

References

[1] X. Li, S.L. Hsu, J. Polym. Sci. Polym. Phys. Ed. 22 (1984) 1331–1342.
[2] J.E. Tanner, J. Chem. Phys. 52 (1970) 2523–2526.
[3] C.E. Hoyle, T.Y. Lee, T. Roper, J. Polym. Sci., Part A: Polym. Chem. 42 (2004) 5301–5338.
[4] K. Shanmuganathan, R.K. Sankhagowit, P. Iyer, C.J. Ellison, Chem. Mater. 23 (2011) 4726–4732.
[5] W.D. Cook, F. Chen, D.W. Pattison, P. Hopson, M. Beaujon, Polym. Int. 56 (2007) 1572–1579.
[6] C.E. Hoyle, C.N. Bowman, Angew. Chem. Int. Ed. 49 (2010) 1540–1573.
[7] M. Uygun, M.A. Tasdelen, Y. Yagci, Macromol. Chem. Phys. 211 (2010) 103–110.
[8] P. Arora, Z. Zhang, Chem. Rev. 104 (2004) 4419–4462.
[9] C.N. Walker, C. Versek, M. Touminen, G.N. Tew, ACS Macro Lett. 1 (2012) 737–741.
[10] S. Suarez, S. Greenbaum, Chem. Rec. 10 (2010) 377–393.
[11] X. Wu, W. Deng, J. Qian, Y. Cao, X. Ai, H. Yang, J. Mater. Chem. A 1 (2013) 10130–10134.
[12] L. Wang, Y. Lu, J. Liu, M. Xu, J. Cheng, D. Zhang, J.B. Goodenough, Angew. Chem. Int. Ed. 52 (2013) 1964–1967.
[13] Y. Lu, J.B. Goodenough, Y. Kim, J. Am. Chem. Soc. 133 (2011) 5756–5759.
[14] H.J.M. Bowen, et al., Tables of Interatomic Distances and Configuration in Molecules and Ions, Special Publication No. 11, The Chemical Society, London, UK, 1958.
[15] F. Rodriguez, C. Cohen, K.C. Ober, A.L. Archer, Principles of Polymer Systems, fifth ed., CRC Press, Ithaca, NY, 2003.
[16] K.-S. Park, S.B. Schougaard, J.B. Goodenough, Adv. Mater. 19 (2007) 848–851.
[17] K.-S. Park, A. Benayad, M.S. Park, A. Yamada, S.G. Doo, Chem. Commun. 46 (2010) 2572–2574.